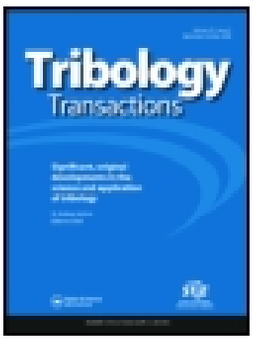

Tribology Transactions

ISSN: 1040-2004 (Print) 1547-397X (Online) Journal homepage: https://www.tandfonline.com/loi/utrb20

Representative Tribometer Testing of Wire Rope Fretting Contacts: The Effect of Lubrication on Fretting Wear

C. J. Dyson, R. J. Chittenden, M. Priest, M. F. Fox & W. A. Hopkins

To cite this article: C. J. Dyson, R. J. Chittenden, M. Priest, M. F. Fox & W. A. Hopkins (2020): Representative Tribometer Testing of Wire Rope Fretting Contacts: The Effect of Lubrication on Fretting Wear, Tribology Transactions, DOI: 10.1080/10402004.2020.1733154

To link to this article: https://doi.org/10.1080/10402004.2020.1733154

Accepted author version posted online: 21 Feb 2020.
Published online: 30 Mar 2020.

TRIBOLOGY TRANSACTIONS
https://doi.org/10.1080/10402004.2020.1733154

Representative Tribometer Testing of Wire Rope Fretting Contacts: The Effect of Lubrication on Fretting Wear

C. J. Dyson[a], R. J. Chittenden[b], M. Priest[c], M. F. Fox[c], and W. A. Hopkins[a]

[a]ITW ROCOL Lubricants, Swillington, Leeds, UK; [b]School of Mechanical Engineering, University of Leeds, Leeds, UK; [c]Faculty of En, University of Bradford, Bradford, UK

ABSTRACT

Fretting wear has a significant influence on wire rope fatigue life when in cyclic bending, particularly for crossed wire contacts, where the interfacial motion of the surfaces is complex and multiaxial. To simulate these contacts in a controlled manner, a laboratory-scale, crossed cylinder, reciprocating fretting wear test was developed. A broad range of contemporary lubrication technologies were evaluated using this method, and a systematic multivariate statistical analysis was performed to identify the most significant lubrication-related parameters with respect to these fretting wear conditions. Wear area increase per slip cycle was the most relevant measure of wear damage, because this captured the influence of changes in the fretting wear regime during the test. The ability of a lubricant to reduce damaging fretting wear during the running-in phase was the greatest influence on long-term fretting wear, particularly for grease-lubricated contacts.

ARTICLE HISTORY
Received 17 October 2019
Accepted 17 February 2020

KEYWORDS
Wire rope; fretting wear; lubrication; lubricants; running-in

Introduction

A key limitation to the life of a wire rope is the accumulated fatigue failure of its individual constituent wires. This is of particular concern for ropes carried over sheaves and pulleys and through fairleads, etc., as part of their operation, where the stress and strain amplitudes are greater than those for static ropes. Accumulation of rope fatigue damage is most critical when operations have a high number of bending cycles, leading to bend fatigue. Fatigue failure of a wire rope typically manifests as broken individual wires with classical flat fracture surfaces without necking *(1)*. Various industry standards set specification criteria for discarding ropes showing a number of visible wire breaks in a given length *(2–5)*. However, peak stresses are found for the inner wires *(6)*, and studies of wire ropes in service indicate that individual wire breaks are not always visible; therefore, external observations may not give an accurate assessment of the bending fatigue response of a rope *(1, 3, 7)*. The contact interfaces between the individual wires in a rope are crucial to bending fatigue performance, generally considered in two categories:

1. Parallel contacts between wires within strands and within structural cables *(8)*.
2. Crossed contacts between wires in adjacent strands. Nabijou and Hobbs *(9)* show that these can be the locations of greatest internal displacement during bending.

When these interfaces are unused, they can be considered as cylinder-on-cylinder contacts, where contact pressures are reported to be extremely high *(6, 10, 11)*, particularly so at crossed contacts where reported values of Hertzian contact pressure range from $P_{max} = 1.05$ to 3.75 GPa and $P_{mean} = 2.5$ GPa *(12–16)*. When the rope is tensioned and then relaxed, twisted, and bent, the individual wires move over each other at these interfaces, causing friction and wear.

These interfaces can wear rapidly initially *(12, 13, 17)*, reducing wire center-to-center distances, rope diameter, etc. *(8, 15, 18–20)*. As wear increases, contact pressures decrease and a steady-state wear regime can be reached *(12, 13, 17)*. Therefore, a controlled running-in process is recommended by rope manufacturers and industry regulations to avoid early damage to these interfaces and maximize rope life *(4, 21, 22)*. These dimensional changes, along with hysteresis in operation, can cause interwire contact areas to shift from their initial locations, which can manifest as a small initial wear scar adjacent to the main location of fretting wear *(23)* (see Fig. 1a). Because the oscillation amplitude has similar orders of magnitude to the contact area, wear particles have little opportunity to be ejected, and these interfaces exhibit fretting wear.

Classical fretting has three regimes, though there are various terms used to describe them *(24–26)*: stick/limited slip (negligible relative motion at the interface), partial slip, and slip (the whole of the interface is in relative motion).

All of these regimes occur at the crossed wire interfaces of a rope *(14, 21, 27–31)*. However, it is not unusual for the interfaces in static ropes to be in the full slip regime. For

CONTACT C. J. Dyson chris.dyson@rocol.com
Review led by M. Dube.

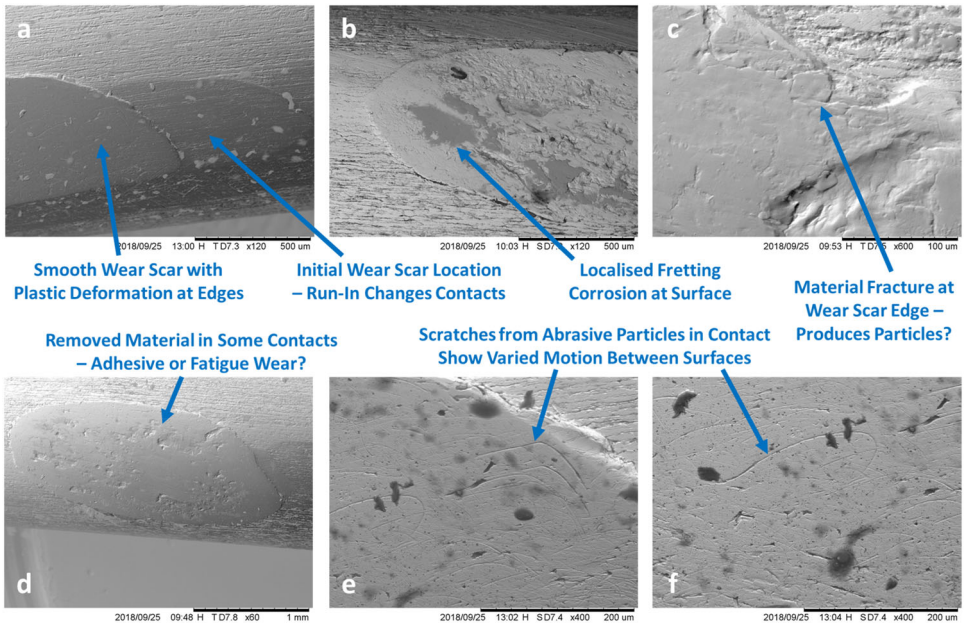

Figure 1. Wear scar images from a winch rope taken out of service.

dynamic ropes, such as winches, etc., where interstrand displacements are higher, it can be assumed that the full slip regime is predominant.

Most classical fretting experiments have uniaxial motion. However, the complex interactions of tension, twist, bending, and straightening that individual crossed wire interfaces experience mean that their motion is rarely uniaxial. For example, Fig. 1 shows a contact area from a crossed wire interface in a winch rope of 30 mm diameter (6×7 right lang lay first layer, 8×26 right regular lay outer layer), with wire diameters 0.3–1.0 mm, taken out of service after exceeding the discard criteria for visible wire fatigue breaks. Fretting wear, corrosion, and plastic deformation can be observed in Figs. 1b–1d. The surface scratches caused by either wear particles or abrasive debris in Figs. 1e–1f show that their motion through the contact follows convoluted paths, indicating multi-axial displacement of the interfaces at an interstrand contact.

At the crossed wire contacts, fretting wear concentrates stresses in these regions through three predominant mechanisms:

1. The cross-sectional area of the wires reduces, concentrating tensile and bending stresses in these worn regions *(14, 32)*.
2. Between regions of stick/limited slip and regions of slip, high frictional stress gradients can exist. Fatigue cracks have been shown to initiate at these boundary regions *(33, 34)*.
3. Because wear particles are often retained in fretting wear contacts, rough wear areas can be produced that allow further concentration of these stresses *(34)*. Therefore, if a contact is in the full slip fretting regime, wear particles are more likely to be removed and thus stress concentration can be reduced. Therefore, if poor lubrication either increases the wear rate or keeps the contact in the stick or partial slip fretting regime, the rate of fatigue failure can increase. Conversely, Waterhouse and Taylor *(34)* and Jin et al. *(35)* observed that the coverage of the interface and embedment/sintering of wear particles can promote slip and reduce stress concentrations.

As such, several studies have identified that these crossed wire contact areas are often the initiation points for fatigue cracks and, ultimately, fatigue breakage of wires *(36, 37)* and are typically square-edged, occasionally propagating to other fatigue cracks in other nearby contacts *(1, 38)*. Harris et al. *(36)* described surface cracks in fretting wear scars as "[assisting] the initiation of fatigue cracks in the wires, Page 70." Waterhouse and Taylor *(34)* reported that the influence of fretting can greatly reduce the fatigue strength of a wire steel.

An oxide layer and martensite formation are observed at these interfaces *(1, 7, 13, 21, 39)*. Furthermore, fretting wear continually regenerates nascent metal surfaces, which, in a corrosive environment, can increase the corrosive wear rate in the crossed wire contact areas. Synergy between mechanical and corrosive wear in fretting can produce wear rates greater than either individual mechanism *(21, 40)*.

Effective lubricants play a significant role in extending wire rope life, for both manufacturing lubricants and aftermarket dressing lubricants. The important functions of a good wire rope lubricant are control of fretting wear and protection against corrosion *(4, 32, 41)*. Waterhouse, referring to proprietary manufacturing lubricants, describes the best lubricants as requiring a high drop point, low unworked penetration, high shear strength, resistance to shear (low increase in penetration on working), and a high value of shear strength in an extrusion test *(42)*. Chaplin and Potts, referring to wax, petrolatum, and bituminous oil-based lubricants, reported that lubricants with a drop point

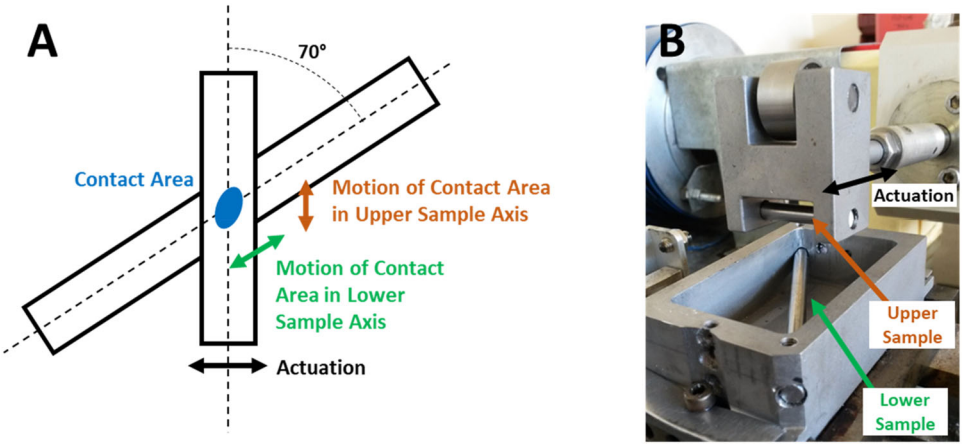

Figure 2. Fretting wear test geometry: (A) schematic and (B) photograph of test equipment.

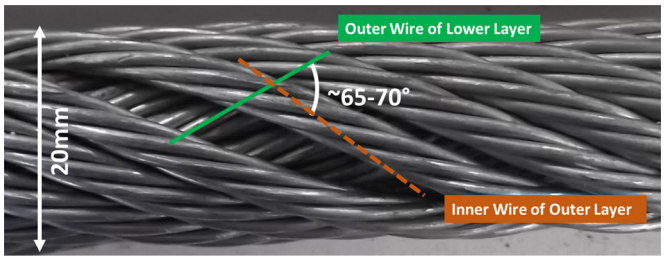

Figure 3. Image of a low-rotation lang lay rope showing the contact angles at interstrand locations.

Table 1. Composition of BS 1407 steel test samples.

Chemical analysis	wt%
Carbon	1.10–1.20
Manganese	0.25–0.45
Silicon	0.00–0.40
Sulfur	0.00–0.035
Phosphorous	0.00–0.035
Chromium	0.35–0.50

>80 °C, unworked penetration <80, and a low increase in penetration on working are the most beneficial *(21)*.

For fretting contacts, friction has less importance to system performance than wear. However, the fretting regimes of crossed wire contacts can have a significant effect on the friction coefficient, which, when aggregated over all of the contacts in a wire rope, has a measurable effect on the elastic response and stiffness of the rope *(31, 43)*.

Various test methods have been reported with regard to wire rope fretting contacts. Some used wires crossed at 90° *(12, 14, 26, 32, 39, 44–46)*, others varied the crossing angle *(6, 13, 47–49)*, and others applied torsional displacement *(49)*. Some used small wires *(6, 12, 14, 32, 37, 47, 49)* and others used large ones; for example, Perier et al. *(39)* used 5.3-mm-diameter rods, McColl et al. *(44)* used 2.8-mm-diameter rods, Waterhouse et al. *(46)* used 2.8- and 5.0-mm-diameter rods, and others ground flat surfaces onto wires *(34)*. Some were unlubricated *(12, 14, 26, 34, 37, 46)*, whereas others used model lubricants *(21, 42, 44)*, commercially available lubricants *(45)*, or model environmental fluids *(49)*. Others observed effects in the early stages of fretting from residual drawing lubricant on the wires *(44, 46)*, and some tests considered fretting fatigue failure by tensioning one of the wires *(37, 47, 49)*. All of these studies had the contact area translated over one surface but concentrated in one location on the other. Though some studies have considered lubricants, there is a need for a broad survey of lubricant-related parameters to identify key performance parameters that can affect fretting wear.

This study has developed and validated a representative fretting wear test designed to investigate lubrication effects on fretting wear. In particular, the translation of the contact area across both surfaces was an important design parameter to simulate contacts observed in the field. This was then systematically applied to investigate key lubrication and tribological parameters that affect fretting wear at these interfaces.

Tribometer test method

A crossed cylinder contact adaptor was developed for a standard commercial reciprocating friction and wear tester, in this case a Phoenix Tribology TE77. To reproduce the multi-axial motion of the contact patch, 5-mm-diameter steel rods were oriented at 70° (see Fig. 2). This angle is typical of the interstrand contact angles within wire ropes. An example is shown in Fig. 3. As with contacts between wire strands in adjacent layers, translation of the contact area on one surface was greater than on the other. The applied displacement amplitude was 35 μm in the upper sample holder axis (a nonstandard displacement), which produced a maximum displacement of 37 μm in the axis of the lower sample and 13 μm in that of the upper sample (Fig. 2A) based on the geometry. Due to some of the strain energy being elastically absorbed by the contacting components, displacement at the interface of a fretting contact was not the same as the applied displacement *(12, 24, 50)*. However, due to the multi-axial motion, it was not possible to measure the real displacement at the interface in this apparatus.

The test samples were turned and polished rods of BS 1407 tool steel; their composition is given in Table 1. Like wire rope steels, this steel can be work-hardened, although it has a higher carbon content than is typical for a wire rope steel. The yield stress of this grade of steel is lower than that of a typical wire rope steel. Referring to the Von Mises yield

criteria (51), the contact stresses will be within experimental variation of the yield stress of the steel; that is, there may be some yielding. The yield stress will certainly be exceeded as soon as interfacial motion occurs. Therefore, the initial contact pressures reported here are considered representative only of the initial static conditions. Preliminary tests did not show excessive plastic deformation early in tests, such as that observed by Atkins and Tabor (52).

In preliminary testing, the observed wear phenomena and mechanisms were comparable to those reported in lubricated wire rope steel contacts in the laboratory (45) and in the field (3, 42). As with rope wire steel (36), the microstructure of BS 1407 steel is typically pearlitic but will not be as highly oriented as drawn wire. For unlubricated drawn wire, Cruzado et al. (13) reported no significant difference in the wear coefficient and energy-specific wear rate with contact angle at the same contact pressure. Therefore, though the residual stress and highly oriented microstructure have been shown to have a significant effect on fretting-related fatigue (42), the effect in these conditions where fretting wear is emphasized was expected to be less significant. Parametric testing indicated that a representative contact could be produced using a normal load of 30 N, which, using Williams and Dwyer-Joyce's Hertzian contact analysis of angled cylinders (53), gave an initial Hertzian maximum contact pressure, P_{max}, of 3.3 GPa and an initial average contact pressure, P_{mean}, of 2.2 GPa. These are representative of contact pressures used in other studies (12, 14, 17, 48). With reference to Fig. 1, where sliding distances of ~0.18 mm in a ~2.0-mm-long contact give a ratio of ~0.09, the scale of the tribometer testing is comparable to sliding distances up to ~0.037 mm in a ~0.5-mm-long contact give a ratio ~0.07.

In parametric testing, rods of various diameters were evaluated under the same contact pressure. Five-millimeter-diameter rods were found to be optimal, because those of significantly lower diameter were found to deform too greatly under load. In some cases, this meant that the contact became concentrated in location on one of the surfaces, which was not representative of the multi-axial motion.

Tests were run for 8 h at 30 Hz, ~850,000 cycles, at ambient temperatures of 15–25 °C. Though 30 Hz is a higher frequency than normal operation for a rope, this gave accelerated testing to a high numbers of cycles, an approach taken in other accelerated fretting studies (46). Because these were fretting contacts where frictional energy dissipation was relatively low, no significant temperature buildup in the near-contact region of the samples was observed. Certainly, near-contact temperatures did not reach the levels seen in worked regions of active heave compensation units where bulk temperatures up to 150 °C have been reported (54), which is close to, or above, the dropping point of some greases (7, 54). No thermal/oxidative degradation of the lubricants was observed in the near-contact area. Before the test was begun, ~2 g of lubricant was applied to the contact area so that the contact area was completely encapsulated.

Friction force and thereby friction coefficient measurements were taken throughout the tests, but these can only be considered as relative indicators of contact behavior because

- the friction force transducer was in the axis of applied displacement, not the actual displacement of the contact in the crossed cylinder configuration, due to the movement of the contact location in different axes across both surfaces and
- the friction force measurement also includes the strain energy stored elastically in the system, with a high value of measured friction coefficient often indicative that the contact was in the stick/limited slip regime.

Friction coefficient measurements were recorded on a 10 s average basis. Recorded friction coefficient measurements reported for a particular test time are the average of the preceding 100 s of data, with the exception of 60 s after the test start when a single 10 s value was reported.

As noted above, parametric testing indicated that high friction coefficient measurements in some tests often correlated with small wear scars and therefore little relative motion between the surfaces, indicating that in these tests the fretting contact was in the stick or partial slip regime, with much of the input energy dissipated elastically. Surfaces observed from a test ended after 21,600 cycles, during running-in and still in the stick/limited slip regime, showed that there was some limited motion at the interface but that there was extensive stick. Strain energy was released by cracking of the subsurface, leading to the formation of wear particles (Fig. 4), which produced galling and plastic deformation of the counterface. This shows the extreme nature of running-in processes under these conditions. By the generalized rules of Hamilton (55), the stick/limited slip regime observed here represents conditions where the maximum yield parameter was at the contact surface. For the slip regime observed in other tests, the maximum yield parameter was significantly reduced from that in the stick/limited slip regime and would have been in the subsurface; some of the differences in wear mechanisms observed indicate this effect.

The stick/limited slip observed was caused by the initial contact area being very small and, once any lubricant in this area was consumed or pushed out, the low entrainment conditions meant that the lubricant supply to the contact ceased, keeping the contact in stick or partial slip conditions. This is typical of fretting contacts. However, this is clearly not representative of wire rope contacts in service, where the duty cycle of ropes bent over sheaves and through fairleads imposes sufficient relative motion between wires to ensure the flow of lubricant, if available, and keep surfaces moving, even under great resistance.

To replenish the lubricant in the contact, the contact surfaces were first separated after 30 min (~54,000 cycles) after the start of the test and then after every hour (~108,000 cycles) of testing and relocated, without removal from the sample holders or with any intervention to the lubricant on or around the contact. The extension of the lubricant as the surfaces parted allowed the lubricant to reflow into the

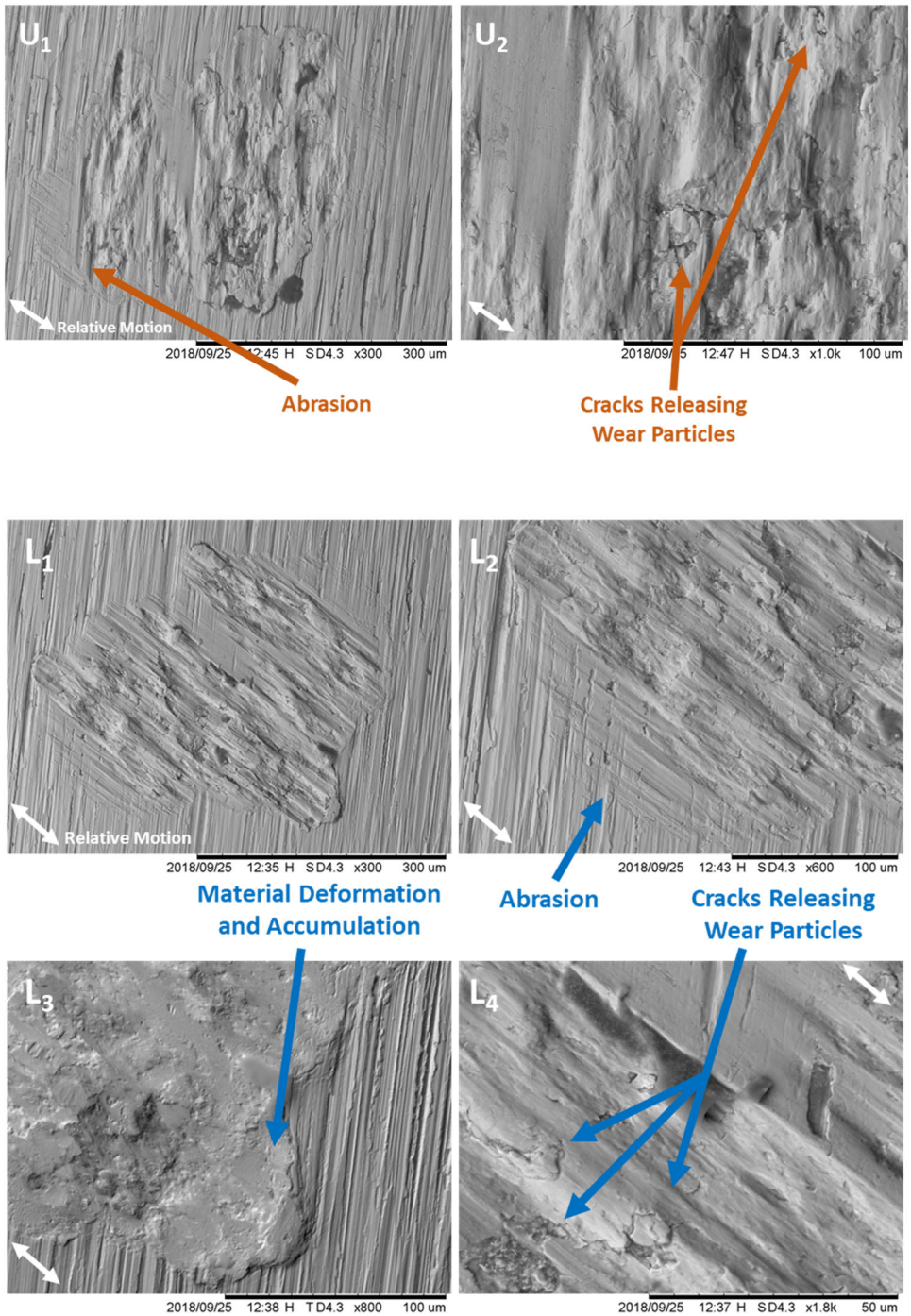

Figure 4. Wear scar images from limited slip regime: U_1–U_2, upper sample; L_1–L_4, lower sample.

contact areas. Observations of the wear scars afterwards showed no duplicated wear scars, misalignment, etc., which confirms the accuracy of the sample holder and loading mechanism and that there was only one contact site. The relative motion in both sample axes assisted this realignment. The effect of this intervention was that some lubricants previous operating in the stick/limited slip regime had more realistic running-in processes that eventually led to full slip, indicated by a significant reduction in the friction coefficient measurement (Fig. 5). For most tests, there was a progressive change in friction coefficient measurement (Fig. 5), which indicated the progression of the slip. For a few tests, full slip occurred immediately after a test was resumed; for others, the lubrication performance was sufficiently poor that the slip regime was never reached. Periodically parting the samples was not ideal tribological practice but improved the correlation with tribological phenomena in the field and improved the repeatability of the test.

When a test began in the stick/limited slip regime and ended in the slip regime, the number of cycles before the friction coefficient measurement began its final reduction toward the steady-state slip condition was recorded. The number of cycles at which the friction coefficient measurement reached a steady-state slip condition was also

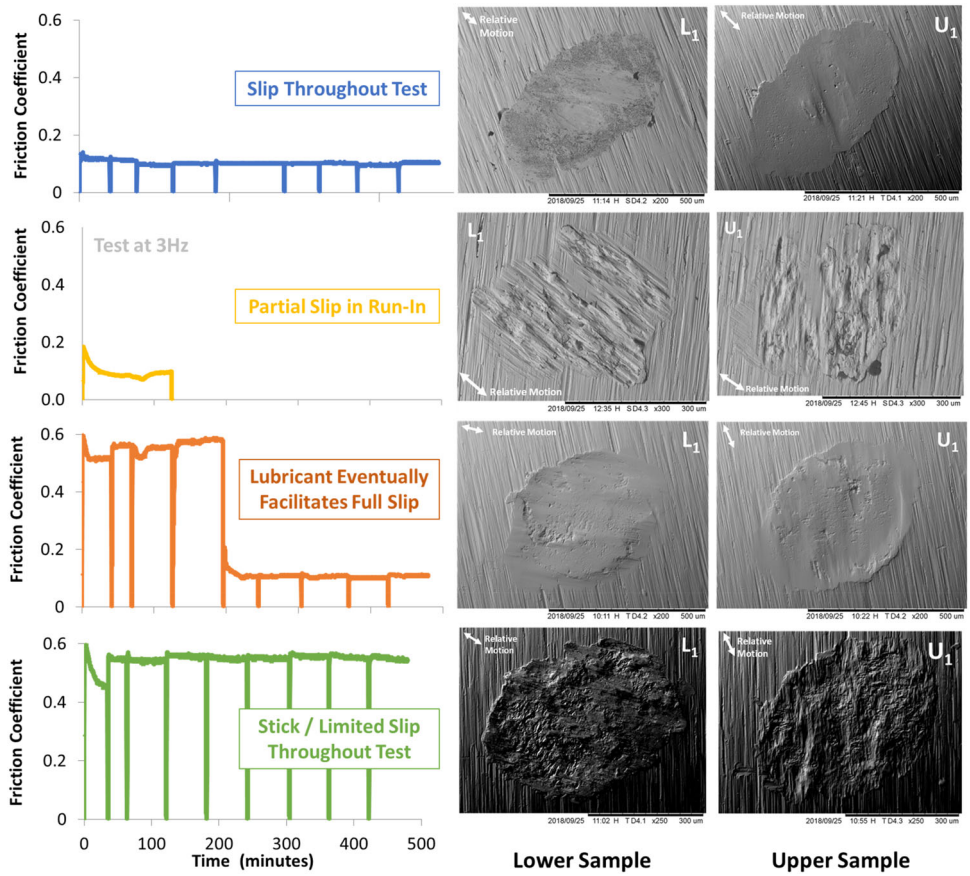

Figure 5. Example friction coefficient traces showing changes in fretting wear regime.

Table 2. Fretting wear test parameters.

Parameter	Value
Rod diameter	5 mm
Theoretical maximum oscillation amplitude	35 μm
Projected maximum oscillation amplitude:	
Upper rod	13 μm
Lower rod	37 μm
Normal load	30 N
Initial maximum Hertzian contact pressure (P_{max})	3.3 GPa
Initial mean Hertzian contact pressure (P_{mean})	2.2 GPa
Theoretical initial Hertzian contact area	1.37×10^{-8} m^2
Translated Hertzian contact area in the sample axis:	
Upper rod	1.49×10^{-8} m^2
Lower rod	1.73×10^{-8} m^2
Oscillation frequency	30 Hz
Test temperature	Ambient ~15–25 °C
Test duration	8 h ~850,000 cycles

recorded. These were used to describe three stages in the tests: the number of cycles before slip begins; the number of cycles when slip is being established; and the number of cycles in the steady-state slip regime. The wear was quantified posttest using two key parameters:

- Wear area increase (WAI) is the area of the wear scar, subtracting the initial Hertzian contact area translated over the surface by the theoretical full displacement (a simplified zero-wear condition).
- Wear area increase per slip cycle (WAISC) is the wear area increase, as above, divided by the number of cycles that the contact spent in the slip regime, as indicated by the friction coefficient measurements.

Tests were conducted at least twice for each lubricant and the statistical significance is given with reference to the standard deviation for each test condition. The design of the test program is given in Table 2. Samples were parted and relocated after 30 min (~54,000 cycles) and then after every hour (~108,000 cycles) up to 7 h after the start of the test, with a total test duration of 8 h.

Effect of lubrication properties on wear

Test matrix

A variety of commercially available greases were evaluated using this test method. Some of these were designed to be wire rope lubricants (manufacturing lubricants and dressing lubricants); others were general-purpose bearing greases and open-gear greases:. These were selected to cover a wide range of representative properties and technologies. The greases were characterized in a variety of ways so that, posttest, key lubricant properties could be evaluated in terms of their influence on wear. The lubricant properties were measured and variable ranges established as shown in Table 3.

A variety of wax-based lubricants were also evaluated. Some were designed to be manufacturing lubricants for wire ropes, and others were designed for different industrial systems. These are different in nature and purpose from

Table 3. Key test grease parameters and their range within this study.

Variable	Test method	Unit	Value range
Kinematic viscosity of base fluid at 40 °C	ASTM D445	cSt	95, 99, 150, 159, 164, 173, 239, 254, 298, 316, 320, 320, 465, 520, 675, 2,174
Kinematic viscosity of base fluid at 100 °C	ASTM D445	cSt	13.0, 13.4, 14.3, 14.7, 15.7, 19.9, 21.8, 22.0, 22.0, 22.7, 23.6, 32.4, 34.9, 35.0, 55.5, 105
Oil separation	ASTM D1742 (40 °C, 168 h)	wt%	0.1, 0.9, 1.0, 1.6, 1.9, 2.3, 2.6, 3.9, 6.1, 7.2, 8.3, 8.5, 9.6, 18.8, 21.6, 31.9
Unworked cone penetration	ASTM D217 (0 strokes)	0.1 mm	166, 243, 244, 276, 277, 280, 280, 280, 292, 298, 303, 303, 325, 360, 365, 456
Worked cone penetration	ASTM D217 (60 strokes)	0.1 mm	244, 255, 274, 280, 280, 283, 300, 300, 303, 313, 325, 325, 348, 366, 370, 420
Four-ball wear scar diameter	ASTM D2266 (40 kg, 60 min)	mm	0.49, 0.63, 0.64, 0.73, 0.74, 0.76, 0.77, 0.78, 0.82, 0.83, 0.85, 0.87, 0.94, 0.99, 1.03, 1.04
Base oil type	—	—	Mineral oil, polyalphaolefin, polybutene, vegetable oil, synthetic ester, mineral wax
Thickener type	—	—	Lithium soap, lithium complex soap, calcium soap, organically modified clay, silica, polymer, hybrid

Table 4. Key wax-based lubricant parameters and their range within this study.

Variable	Unit	Value range
Melting point	°C	60–85
Wax content	%	Proprietary
Base oil type	—	Mineral wax, residual oil, natural oil/wax
Additives	—	Base wax only, antiwear additives

greases, where some parameters relevant to greases are not applicable, such as base oil viscosity and oil separation, and cone penetration of waxes is generally performed using different test cones that do not correlate well with those for grease *(56–58)*. Therefore, the results from wax-based lubricants were analyzed separately. Information on these waxes is shown in Table 4.

Grease-lubricated systems

Figure 6 shows the wear area increase per slip cycle, and Fig. 7 shows the wear area increase measurements for grease-lubricated contacts, ranked by the wear parameter for the lower sample. There is clear differentiation between those with the lowest wear parameters and those with the highest.

Figure 8 shows the wear scars for a nominally good grease, marked "G" in Figs. 6 and 7. The fretting wear mechanisms shown here are also comparable to other tests with statistically similar values of WAISC. The centers of the wear scars were smooth, with several small pits that could be areas where material was removed earlier in the test, as shown in Fig. 4: The absence of further cracks and adhesive wear features around these suggest that these pits had ceased propagating, showing behavior similar to that observed for adhesive wear pits in rope wire fretting by McColl et al. *(44)*. At the edges of the contacts, the surface appeared to contain a compacted layer of particles, probably wear particles, that had accumulated. There was evidence of this phenomenon at the edge of the contacts in Figs. 1b and 1d, which was also observed in other studies *(13)*. The lack of abrasive wear features suggests that this layer was stable; that is, there was relatively little movement of the particles under shear. The formation in fretting wear of stable surface layers containing embedded/sintered wear particles was observed in other studies and was linked to stable fretting wear conditions *(35, 46, 59)*. Plastic deformation was apparent at the contact edges, as also observed in other studies *(13, 37)*.

Figure 9 shows the wear scars for a nominally poor grease, marked "P" in Figs. 6 and 7. The fretting wear mechanisms shown here are also comparable to those in tests that produced higher values of WAISC. The wear scar appeared to contain a layer of loosely compacted particulates, some of which are wear particles; others may have been ingredients of the lubricant. These particulates also accumulated at the contact edges and, due to the cyclic changes in contact conditions in these regions, appeared to cause abrasive wear. If the loose particulates in the contact center moved under contact stresses, they would be expected to cause significant abrasive wear. The mixture of surface-derived and lubricant-derived particulates may not have permitted a stable layer at the interface and increased the extent of three-body wear. The ejection of these particles from the central contact zone may have caused the abrasion at the contact edges.

Figure 10 shows the wear scars for an intermediate grease that showed inconsistent performance, marked "I" in Figs. 6 and 7. The fretting wear mechanisms shown here are also comparable to other tests with statistically similar values of WAISC. A layer of compacted particles is seen at the center of the wear scar that appeared to have a mixed composition; that is, of both wear particles and ingredients of the grease. At the edges of the contact, extensive surface scratch marks indicated that the wear scars were growing via abrasion. The surface layers in the wear scars did not appear to be stable, and the contacts exhibited three-body fretting–abrasion. Outside of the contact area, particles appear to have built up and were compacted and produced rough worn areas; it is likely that particles accumulated, became concentrated, and were ground between the near-contact regions of the samples. McColl et al. *(44)* observed similar accumulations of lubricant and wear particles around the contact area. The latter effect would not be desirable in a real system, even if the wear parameters of the main contact area were relatively good. The extent of this phenomenon occurring in the field is not known.

From the results for a range of lubricants, it 8s clear that role of the lubricant in forming a stable and wear-resistant

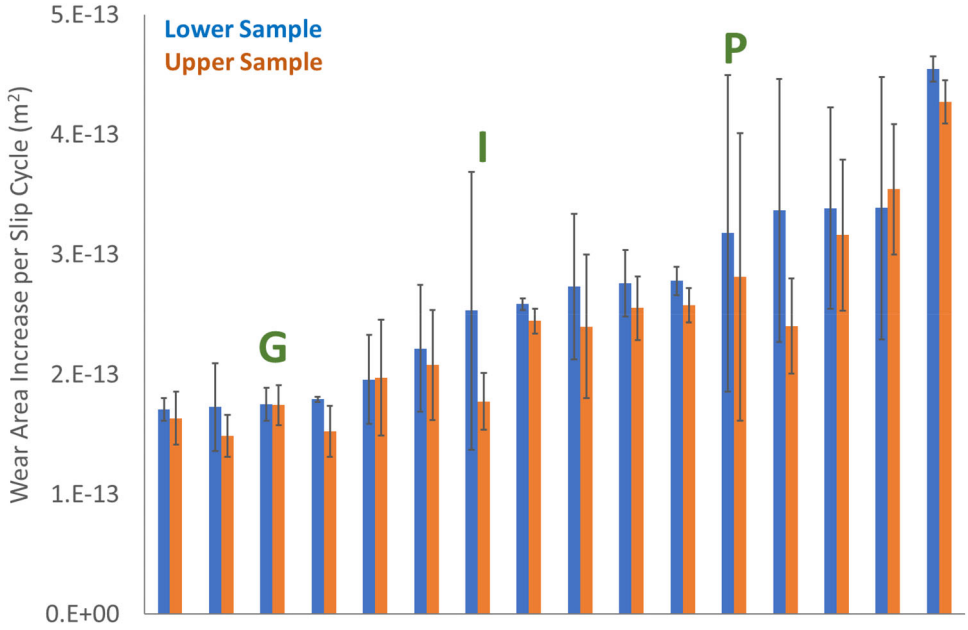

Figure 6. Wear area increase per slip cycle results for grease-lubricated contacts, ranked by wear area increase per slip cycle for the lower sample. G is a nominally good lubricant for which surface analysis is shown in other figures; I is a nominally intermediate lubricant; P is a nominally poor lubricant.

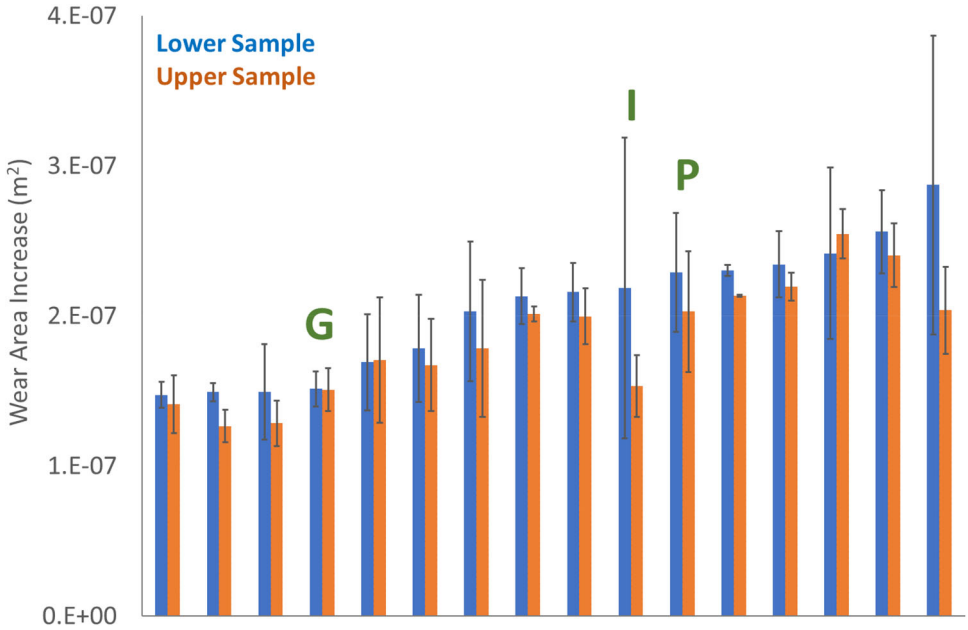

Figure 7. Wear area increase results for grease-lubricated contacts, ranked by wear area increase for the lower sample. G is a nominally good lubricant for which surface analysis is shown in other figures; I is a nominally intermediate lubricant; P is a nominally poor lubricant.

contact surface is critical. Contacts with greater particulate mobility in the interface showed more abrasive wear, resulting in greater long-term wear. These samples showed wear mechanisms representative of other tests with similar results *(13, 14, 32, 37, 39)*. The features observed in these laboratory-scale wear scar tests correlate well with those seen on in-service ropes (Fig. 1).

Regression analysis of grease-lubricated systems

A systematic linear regression analysis of the grease results sought to identify significant trends and factors influencing the wear parameters. Wear area increase and wear area increase per slip cycle were analyzed against the variables in Table 5.

To improve the accuracy of the regression, only one variable was selected from each of the friction coefficient running-in, ambient temperature, cone penetration, and kinematic viscosity categories. This was done with reference to the variable that had the highest Pearson correlation coefficient with the wear parameter under consideration: For both WAI and WAISC these were the friction coefficient after 30 min (μ_{30}), maximum ambient temperature (T_{max}), unworked cone penetration (CP_u), and base oil kinematic viscosity at 40 °C (KV40). As the regression analysis

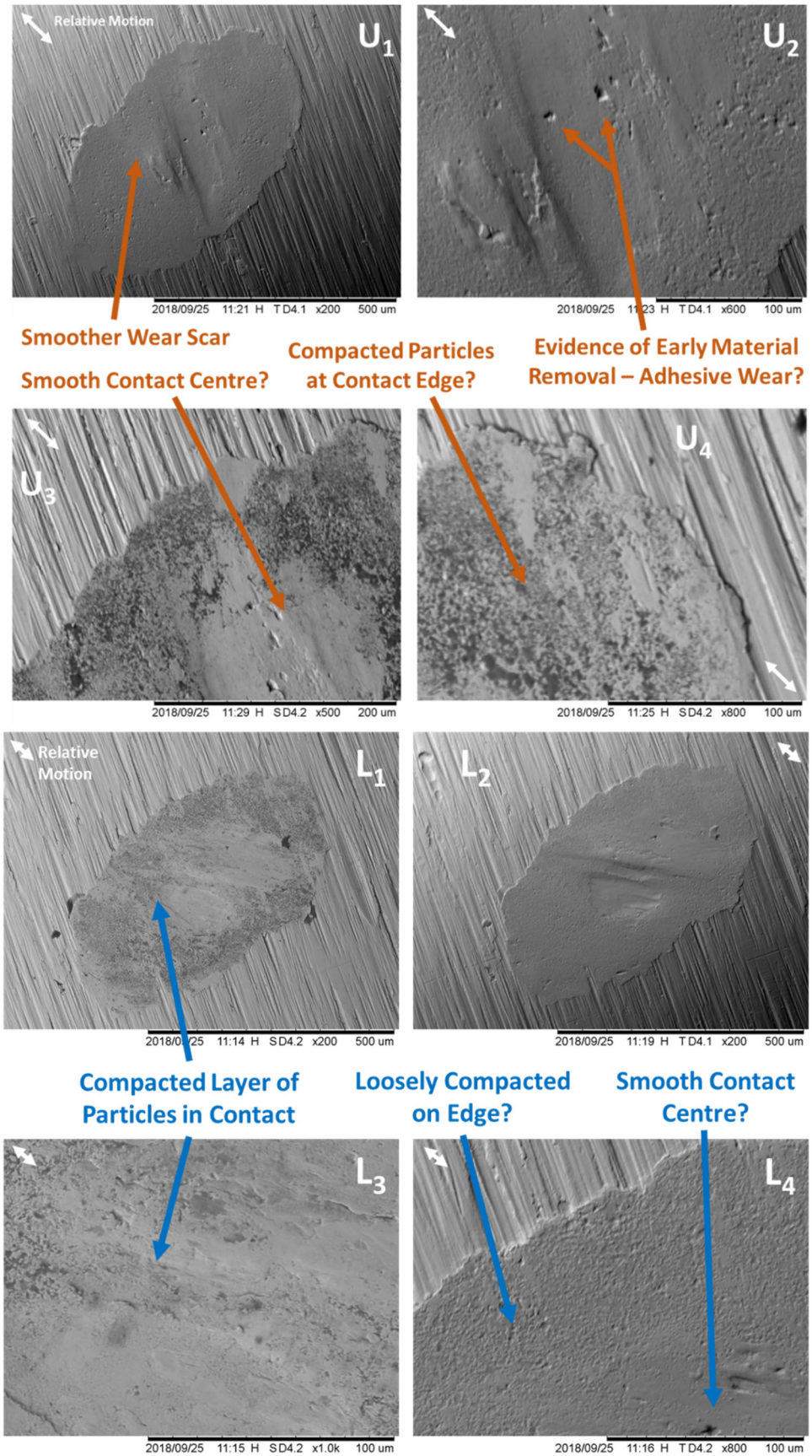

Figure 8. Wear scar images using a good grease: U_1–U_4, upper sample; L_1–L_4, lower sample.

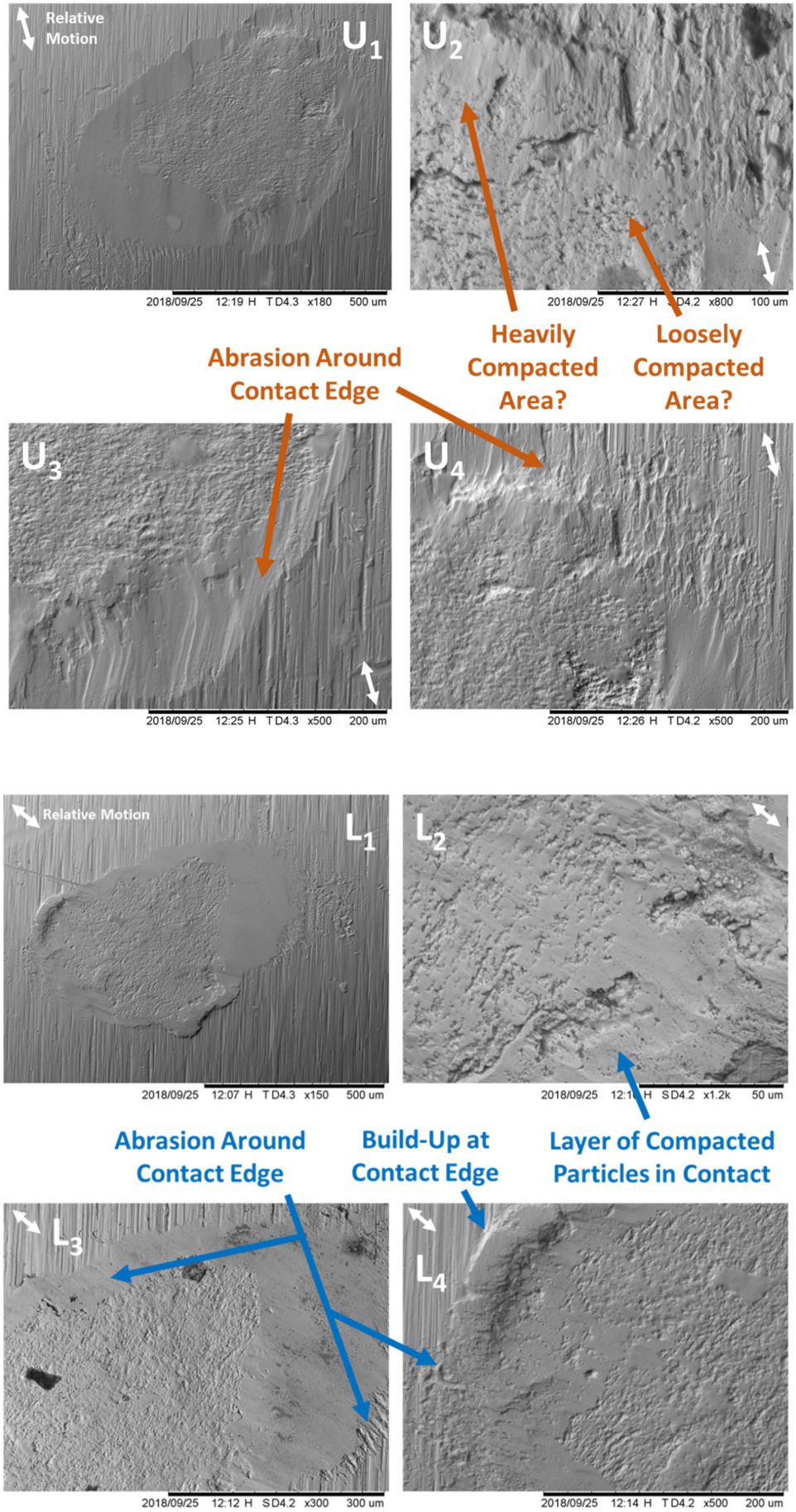

Figure 9. Wear scar images using a poor grease: U_1–U_4, upper sample; L_1–L_4, lower sample.

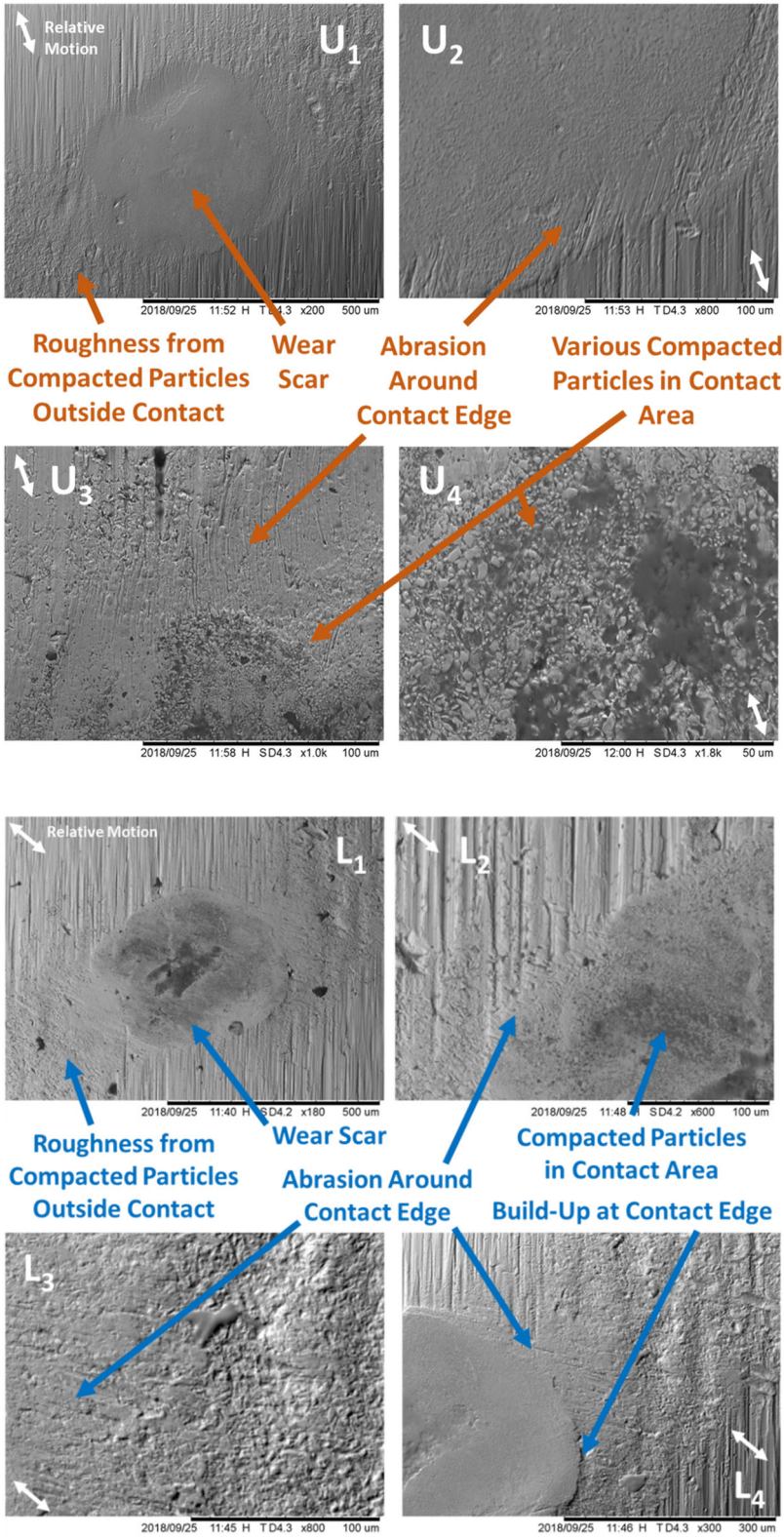

Figure 10. Wear scar images using an intermediate grease: U_1–U_4, upper sample; L_1–L_4, lower sample.

progressed, variables were eliminated until the analysis of variance p-value significance was ≤ 0.05 and the t-values for each coefficient were >1. Regression analyses were undertaken independently for both the upper and lower samples and showed that WAI can be modeled for each by

$$\mathrm{WAI}_{\mathrm{upper}} = 1.66 \times 10^{-7} - (2.50 \times 10^{-11} \times \mathrm{KV40}) + (1.75 \times 10^{-7} \times \mu_{30\mathrm{min}}); R^2 = 0.72 \quad [1]$$

$$\mathrm{WAI}_{\mathrm{lower}} = 1.66 \times 10^{-7} - (2.50 \times 10^{-11} \times \mathrm{KV40}) + (1.75 \times 10^{-7} \times \mu_{30\mathrm{min}}); R^2 = 0.37 \quad [2]$$

Table 5. Input variables considered for linear regression analysis to model fretting wear parameters with grease lubrication.

Parameter		Measurement
Friction coefficient running-in	μ_1	1 min
	μ_{30}	30 min
	μ_{60}	60 min
Friction coefficient steady-state	μ_{SS}	Average of values above that are in the same tribological regime as at the end of the test; that is, full slip, stick/partial slip. Maximum of five values averaged, from the end of the test
Slip establishment (cycles)	N_{stick}	Number of cycles before slip begins to initiate
	$N_{partial}$	Number of cycles while full slip is established
	N_{slip}	Number of cycles in steady-state full slip regime
Ambient temperature	T_{min}	Test minimum
	T_{mean}	Test mean
	T_{max}	Test maximum
Cone penetration	CP_u	Unworked (0 strokes)
	CP_w	Worked (60 strokes)
Oil separation	OS	wt%
Base oil kinematic viscosity	KV40	Kinematic viscosity at 40 °C
	KV100	Kinematic viscosity at 100 °C

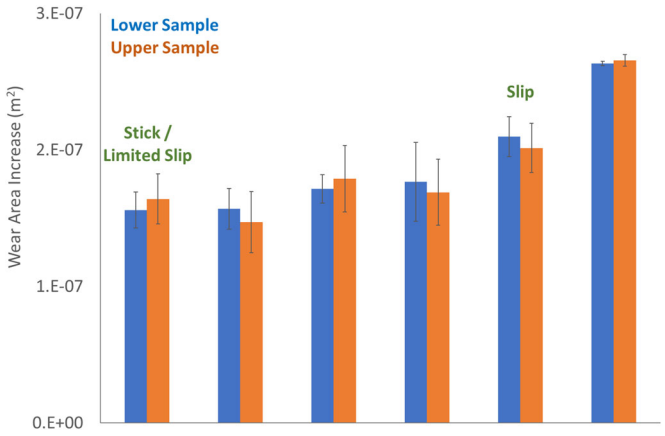

Figure 11. Wear area increase results for wax-lubricated contacts, ranked by wear area increase for the lower sample. Examples with different end-of-test fretting regimes are identified.

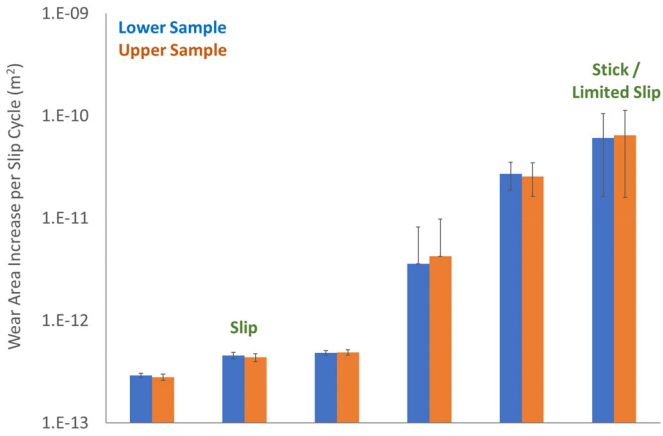

Figure 12. Wear area increase per slip cycle results for grease-lubricated contacts, ranked by wear area increase per slip cycle for the lower sample. Examples with different end-of-test fretting regimes are identified. Note logarithmic y-axis.

where KV40 is the kinematic viscosity (cSt) of the base fluid at 40 °C and μ_{30min} is the coefficient of friction measurement after 30 min (~54,000 cycles) of the test.

Similarly, WAISC can be modeled by

$$\mathrm{WAISC_{upper}} = 1.63 \times 10^{-13} - (3.40 \times 10^{-17} \times \mathrm{KV40}) + (2.10 \times 10^{-13} \times \mu_{30min}) + (7.25 \times 10^{-19} \times N_{stick}); R^2 = 0.89 \quad [3]$$

$$\mathrm{WAISC_{lower}} = 2.02 \times 10^{-13} - (3.10 \times 10^{-17} \times \mathrm{KV40}) + (1.41 \times 10^{-13} \times \mu_{30min}) + (8.19 \times 10^{-19} \times N_{stick}); R^2 = 0.74 \quad [4]$$

where N_{stick} is the number of cycles in the stick/limited slip regime before the transition to the slip regime begins.

The models for wear area increase per slip cycle gave a more accurate description of the tribological system, indicated by the higher values of R^2. The models for the upper and lower samples were generated independently and, predictably, contain the same parameters and similar magnitudes of influence, although with different R^2 values; that is, describing different proportions of the wear parameter variability.

Base fluid kinematic viscosity (KV40) had a significant influence on wear. The inverse relationship, that higher base fluid viscosity reduces wear, appears to contradict established understanding that a lower viscosity base fluid can be more effective in reducing fretting wear because it will more easily bleed from the grease and penetrate into the contact *(60)*. The beneficial effects of lower base fluid viscosity have been observed in oil lubrication as well *(42, 61)*. However, there was not necessarily a contradiction: The ability for lower base fluid viscosity to reduce wear is relevant to fretting wear systems where lubricant supply into the contact more significantly influences behavior. However, in the present system when resetting the test samples regularly reintroduced lubricant to the contact through the test, the ability of the lubricant to flow into the contact was less critical. When lubricant supply to the contact was good, a higher base fluid viscosity could more effectively reduce fretting wear: McColl et al. *(44)* have observed this effect for rope wire fretting, and others have observed the same in fretting wear lubricated with oil alone *(60)*.

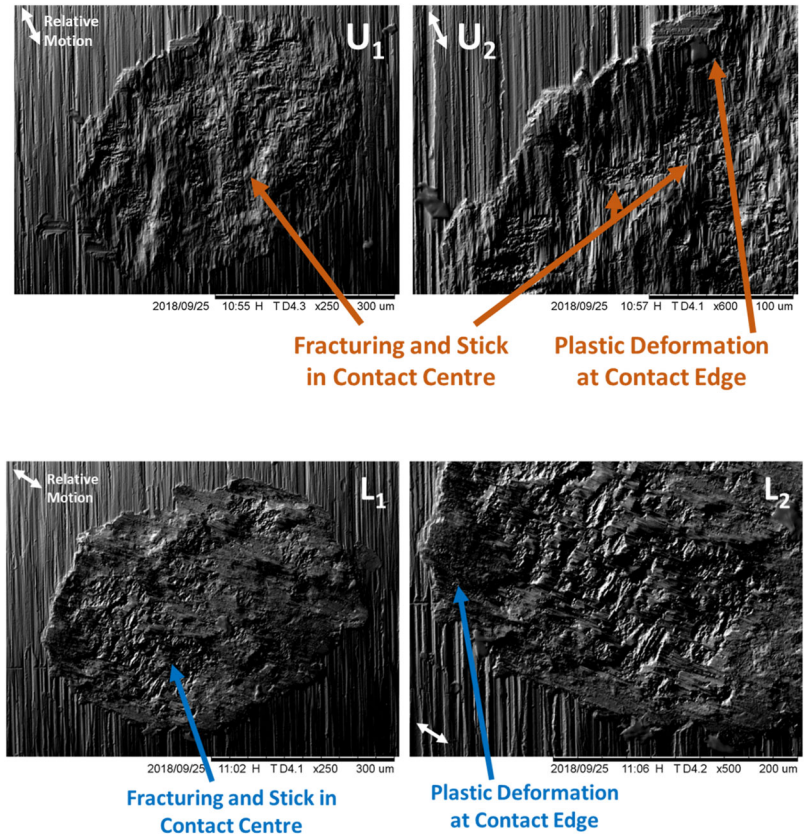

Figure 13. Friction coefficient measurement traces for wax-based lubricants that produce different fretting wear regimes.

The link between the wear parameters, the friction coefficient after 30 min (μ_{30}), and the number of cycles before slip initiation (N_{stick}) was of great importance. These strong influences suggested that the fretting wear regime in the early stages of a test (slip or stick/limited slip) was a key predictor of the fretting wear at the end of the test. Inferring fretting regime changes from friction coefficient measurements (as in Fig. 5), tests where the stick/limited slip regime was predominant early in the test produced greater fretting wear overall. Figure 4 shows that contacts in the stick–limited slip regime during the running-in phase showed severe surface damage. This early damage appears to influence subsequent fretting wear behavior. Providing a controlled running-in stage appeared to be a very important lubricant function with regard to long-term fretting wear and, therefore, maximizing rope life. The wear area images suggest that the difference between effective and less effective lubricants appeared to be the ability to form a stable interface layer (Fig. 8) and to limit the accumulation of loose wear particles, because these caused the longer-term growth of the wear area by abrasion (Fig. 9).

Waterhouse *(42)* described the best lubricants as requiring a high drop point, low unworked penetration, high shear strength, and resistance to shear (low increase in penetration on working) and a high value of shear strength in an extrusion test. Chaplin and Potts *(21)* reported that the lubricant drop point should be >80 °C and unworked penetration <80 (referring to waxes) and that a low increase in penetration on working was beneficial. The results above do not necessarily invalidate these previous studies and, in many respects, reinforce these observations. However, the statistical analysis indicates that the key lubrication parameter was the effect on the running-in of the system. The importance of the positive interaction of the lubricant during running-in surpassed the importance of the lubricant properties identified in previous studies.

Wax-lubricated systems

Figures 11 and 12 show the wear area increase and wear area increase per slip cycle results for wax-lubricated contacts. There was clear differentiation between those with the lowest wear area increase and those with the highest. However, this parameter did not adequately explain this particular data. Figure 13 shows examples of the friction behavior in wax-lubricated tests: All tests began in the stick/limited slip regime. However, some wax lubricants did not provide sufficient lubrication to allow the contact to transition out of the stick/limited slip regime, and others enabled the contact to reach the slip regime. An example from each regime is identified in Figs. 11 and 12. Figure 11 shows that the wear area increase for stick/limited slip tests was lower because the relative motion at the interface was significantly lower.

Figure 12 shows that the wear area increase per slip cycle was more effective in differentiating the fretting wear damage in each regime (cf. Fig. 11). Binary behavior was

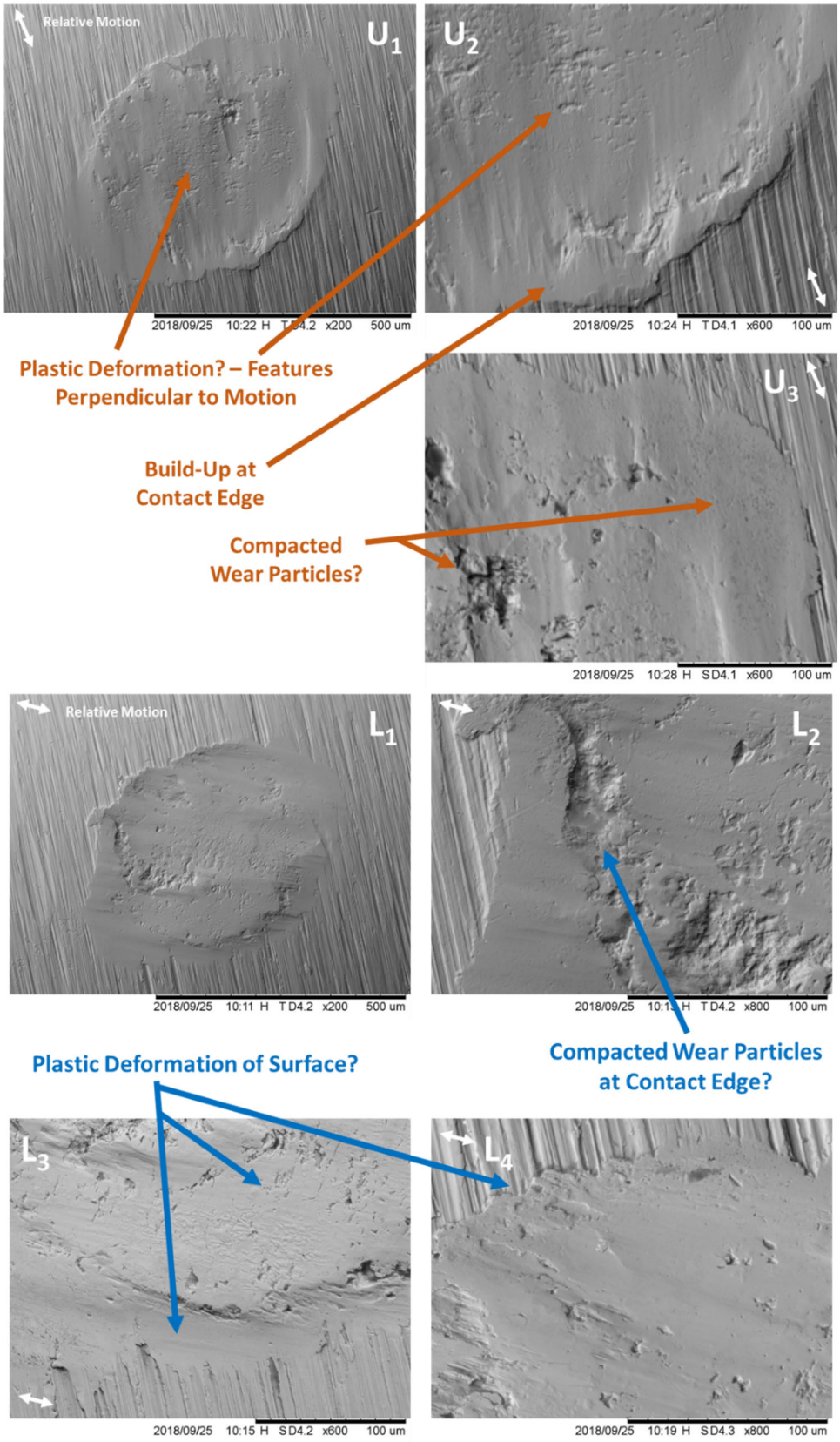

Figure 14. Wear scar images using a wax-based lubricant in the stick/limited slip regime: U_1–U_2, upper sample; L_1–L_2, lower sample.

observed, where the fretting wear damage was significantly higher in the stick/limited slip regime. This illustrates the principle that, in fretting wear, the size of wear scars without reference to the fretting wear regime does not allow suitable interpretation of results. It is important to note that the wear area increase per slip cycle results in Fig. 12 are plotted on a logarithmic axis to improve the clarity of the results.

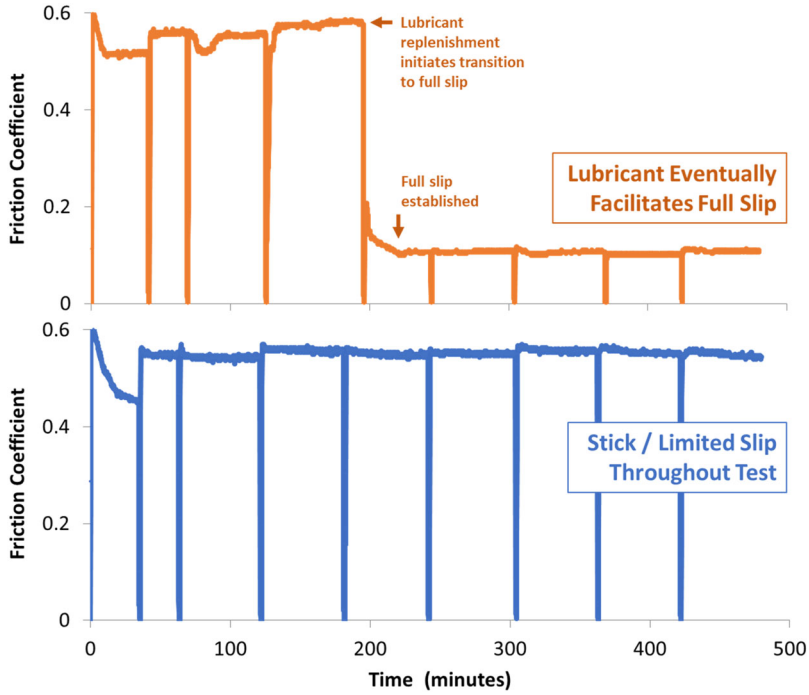

Figure 15. Wear scar images using a wax-based lubricant in the slip regime: U_1–U_3, upper sample; L_1–L_4, lower sample.

Table 6. Input variables used for linear regression analysis to model fretting wear parameters with wax-based lubricants.

Parameter		Measurement
Friction coefficient running-in	μ_{30}	30 min
Friction coefficient steady-state	μ_{SS}	Average of values above that are in the same tribological regime as at the end of the test; that is, full slip, stick/partial slip. Maximum of five values averaged, from the end of the test
Slip establishment (cycles)	N_{before}	Number of cycles before slip begins to initiate
	$N_{partial}$	Number of cycles while full slip is established

Figure 14 shows wear scars for a test where the contact was always in the stick/limited slip regime, marked as "stick/limited slip" in Figs. 11 and 12. Some wear features aligned with the axis of motion, indicating some movement at the interface; that is, limited slip rather than stick. There is a central region of limited slip and an outer region where contact and loading varied with more relative motion and plastic deformation was observed. Because strain energy was not easily dissipated at the interface, stress concentration occurred and cracks formed. These cracks appeared to be at the boundary between the center of the wear scar area and the region of plastic deformation at the edges. Other studies report that cracks can initiate at the boundaries between slip and nonslip regions, where frictional stress gradients are highest *(33)*.

Figure 15 shows wear scars for a test that began in the stick/limited slip regime but that eventually reached the slip regime, marked as "slip" in Figs. 11 and 12. Plastic deformation appears to have occurred throughout the contact area. Wear particles appear to have been compacted into the surface and a stable interface was formed.

Damage to surfaces and subsurfaces was significantly greater when the contact was only in the stick/limited slip regime. Enabling the contact to establish the slip regime appeared to be important for long-term fretting wear control. It is noted that, in bending-over-sheave service, it is unlikely that the stick/limited slip regime could be sustained in the same manner, with the greater tangential stresses and strains forcing the contact displacement at the interface. However, these results suggested that surface and subsurface damage would likely be far more severe with lubricants that do not enable the slip regime to be established in laboratory tests such as these.

Regression analysis for wax systems

As with the results from the grease tests, a systematic regression analysis was performed on the wear area increase per slip cycle data. Because of the smaller number of data points and the fewer measurable properties of these wax lubricants, a smaller set of regression variables was selected (Table 6). The same criteria for analysis of variance p-value significance (≤ 0.05) and t-value (>1) were used as for the grease test results. Initial models produced negative intercepts on the wear parameter axes, so the intercept was set to 0.

Regression analysis showed that WAISC could be modeled by

$$\mathrm{WAISC}_{\mathrm{upper}} = 6.44 \times 10^{-11} \times \mu_{SS}; R^2 = 0.71 \quad [5]$$

$$\mathrm{WAISC}_{\mathrm{lower}} = 6.44 \times 10^{-11} \times \mu_{SS}; R^2 = 0.72, \quad [6]$$

where μ_{SS} is the steady-state friction coefficient.

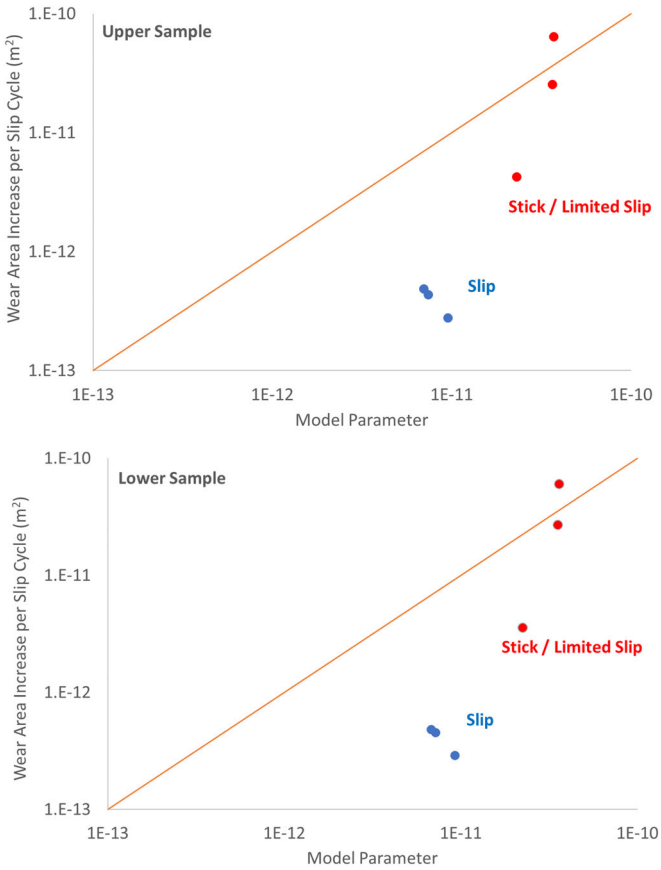

Figure 16. Wear area increase per slip cycle for wax-based lubricants; predicted model from regression compared to experimental results.

These models reflected the bimodal nature of the fretting wear behavior of these wax-based manufacturing lubricants:

- High friction coefficient measurements in the stick/limited slip regime.
- Low friction coefficients in the slip regime.

This can be seen by the groupings of these two behaviors when the experimental data were plotted against the regression model prediction (Fig. 16). All tests began in the stick/limited slip regime, so differentiation in the early stages of the test could not be identified. However, for the slip regime to be established, there may have been significant differences in wear and lubrication phenomena in the running-in phase of the tests, as with the greases. Overall, the ability of the lubricant to produce a stable interface layer and to enable the interface to operate in the slip regime was the most beneficial to long-term fretting wear performance. There is a need for further refinement of the experimental parameters for wax-based manufacturing lubricants. The binary behavior does not seem to fully reflect behavior in the field and, as shown in Fig. 16, the model overpredicts the conditions where the slip regime occurs.

Implications for industry

The controlled running-in of ropes has a significant effect on the overall life of a rope. This study has shown that the lubricant can have a significant influence on the effectiveness of the running-in period and consequently on the long-term fretting wear performance. Clear differentiation has been shown between lubricants that have good and poor performance. Formulators and rope manufacturers should therefore consider both running-in performance and long-term performance when specifying a lubricant.

The optimum base oil viscosity of a wire rope lubricant is dependent on the environment in which it operates; for example, cold artic waters as compared to the temperature of a worked section of an active heave compensation rig, with temperatures up to 150 °C *(54)*. When lubricant supply to the contact affects fretting lubrication performance, the common understanding is that a lower viscosity base oil can be beneficial. However, in the contact, a higher viscosity base oil has been shown to be better at reducing fretting wear. Therefore, an optimum balance of these approaches is needed.

The lubrication performance of some wax-based lubricants was exceptionally poor. If running-in is crucial to rope life, there is scope to improve the lubrication performance of wax-based manufacturing lubricants.

Conclusions

A laboratory-scale fretting wear test was successfully developed to simulate the crossed wire contacts in a wire rope during cyclic bending in service:

- Wear area increase per slip cycle was the most relevant measure of wear damage, because this captured the influence of changes in the fretting wear regime during the test.
- Good lubricants (greases and waxes) allowed a stable interface layer to form, where wear particles were embedded/sintered and where the lubricant reduced adhesive wear without permitting abrasive three-body wear.
- Poor grease lubricants produced loose interfacial layers that caused abrasive three-body wear, particularly at the edges of the contact area.
- Poor wax lubricants did not enable the contact to develop from the stick/limited slip regime.
- Statistical analysis showed that, for greases, the most beneficial factors for long-term fretting wear performance were a higher base oil kinematic viscosity (provided that lubricant supply was suitable) and the ability to reduce damaging fretting wear mechanisms during the running-in phase.

Acknowledgments

A significant amount of the initial feasibility study, design work, and method development for this study was done by project students and summer students at the University of Leeds. We recognize Eduardo Albuquerque Castelo Branco, Tharika Sheyanthini Mohanadasan, Leow Choon Seng, Yanpeng Fu, Daniel Liau, Jack Lyons, Alexander Shaw, Khai Zin Thein, and Tony Wong. We are grateful to Professor Ben

Whiteside at the Centre of Polymer Micro and Nano Technology at the University of Bradford for support with the SEM imaging.

ORCID

M. Priest http://orcid.org/0000-0002-4879-5469

References

(1) Verreet, R. and Ridge, I. (2005), *Wire Rope Forensics*, Kirkel, Germany: Casar Special Wire Ropes.

(2) Chaplin, C. R. and Potts, A. E. (1991), "Discard Criteria for Mooring Ropes," *Wire Rope Offshore—A Critical Review of Wire Rope Endurance Research Affecting Offshore Applications*, , pp 226–264. London, UK: Health and Safety Executive, Marine Technology Directorate Ltd., University of Reading.

(3) Steven, S. (2016), "Validity of Rope Discard Criteria," *MCA Wire Rope Forum Workshop*, 22nd June 2016, Amsterdam, The Netherlands.

(4) Union Wire Rope. (2008), *Wire Rope User's Handbook*, WireCo WorldGroup: Kansas City, MO.

(5) ISO 4309. (2004) "Cranes—Wire Ropes—Care, Maintenance, Installation, Examination and Discard," 3rd Ed. Geneva, Switzerland: ISO.

(6) Wang, D., Zhang, D., Wang, S., and Ge, S. (2013), "Finite Element Analysis of Hoisting Rope and Fretting Wear Evolution and Fatigue Life Estimation of Steel Wires," *Engineering Failure Analysis*, **27**, pp 173–193. doi:10.1016/j.engfailanal.2012.08.014

(7) Saipem. (2016), "Large Wire Ropes," *IMCA Wire Rope Forum Workshop*, 22nd June 2016, Amsterdam, The Netherlands.

(8) Raoof, M. and Kraincanic, I. (1995), Analysis of a Large Diameter Wire Rope," *Journal of Engineering Mechanics*, **121**, pp 667–675. doi:10.1061/(ASCE)0733-9399(1995)121:6(667)

(9) Nabijou, S. and Hobbs, R. E. (1995), "Relative Movements within Wire Ropes Bent over Sheaves," *Journal of Strain Analysis for Engineering Design*, **30**, pp 155–165. doi:10.1243/03093247V302155

(10) Gnanavel, B. K., Gopinath, D., and Parthasarathy, N. S. (2010), "Effect of Friction on Coupled Contact in a Twisted Wire Cable," *Journal of Applied Mathematics*, **77**, pp 024501-1–024501–6.

(11) Kumar, K., Cochran, J. E., Jr, and Cutchins, J. A. (1997), "Contact Stresses in Cables Due to Tension and Torsion," *Journal of Applied Mechanics*, **64**, pp 935–939. doi:10.1115/1.2789002

(12) Cruzado, A., Hartelt, M., Wasche, R., Urchegui, M. A., Gomez, X. (2010), "Fretting Wear of Thin Steel Wires. Part 1: Influence of Contact Pressure," *Wear*, **268**, pp 1409–1416. doi:10.1016/j.wear.2010.02.017

(13) Cruzado, A., Hartelt, M., Wasche, R., Urchegui, M. A., Gomez, X. (2011), "Fretting Wear of Thin Steel Wires. Part 2: Influence of Crossing Angle," *Wear*, **273**, pp 60–69. doi:10.1016/j.wear.2011.04.012

(14) Urchegui, M. A., Martelt, M., Klaffke, D., and Gomez, X. (2007), "Laboratory Fretting Tests with Thin Wire Specimens," *Tribotest*, **13**, pp 67–81. doi:10.1002/tt.34

(15) Argatov, I. (2011), "Response of a Wire Rope Strand to Axial and Torsional Loads: Asymptotic Modeling of the Effect of Interwire Contact Deformations," *International Journal of Solids and Structures*, **48**, pp 1413–1423. doi:10.1016/j.ijsolstr.2011.01.021

(16) Jiang, W.-G., Warby, M. K., and Henshall J. L. (2008), "Statically Indeterminate Contact in Axially Loaded Wire Strand," *European Journal of Mechanics A/Solids*, **27**, pp 69–78. doi:10.1016/j.euromechsol.2007.02.003

(17) Cruzado, A., Urchegui, M. A., and Gomez, X. (2012), "Finite Element Modeling and Experimental Validation of Fretting Wear Scars in Thin Steel Wires," *Wear*, **289**, pp 26–38. doi:10.1016/j.wear.2012.04.018

(18) Miscoe, A. J. and McKewan, W. M. (1993), *Wire Rope Research: Analysis of Bending Fatigue in a 2-Inch IWRC Wire Rope*, Pittburgh, PA, USA: United States Department of the Interior, Bureau of Mines.

(19) Raoof, M. (1990), "Comparison between the Performance of Newly Manufactured and Well-Used Spiral Strands," *Proceedings of the Institution of Civil Engineers Part 2*, **89**, pp 103–120. doi:10.1680/iicep.1990.5254

(20) Chaplin, C. R. and Potts, A. E. (1991), "Inspection of Mooring Ropes," *Wire Rope Offshore—A Critical Review of Wire Rope Endurance Research Affecting Offshore Applications*, pp 265–288. London, UK: Health and Safety Executive, Marine Technology Directorate Ltd., University of Reading.

(21) Chaplin, C. R. and Potts, A. E. (1991), "Corrosion Effects on Mooring Ropes," *Wire Rope Offshore—A Critical Review of Wire Rope Endurance Research Affecting Offshore Applications*, pp 182–225. London, UK: Health and Safety Executive, Marine Technology Directorate Ltd., University of Reading.

(22) Wirerope Works Inc. (2008), *Rotation-Resistant Wire Rope*, Williamsport, PA: Wirerope Works Inc.

(23) Boniardi, M., Cincera, S., D-Errico, F., and Tagliabue, C. (2007), "Fretting Phenomena on an All Aluminium Alloy Conductor," *Key Engineering Materials*, **348–349**, pp 5–8. doi:10.4028/www.scientific.net/KEM.348-349.5

(24) Fouvry, S., Kapsa, P., and Vincent, L. (2003), "A Global Methodology to Quantify Fretting Damages," *Fretting Fatigue: Advances in Basic Understanding and Applications*, Mutoh, Y., Kinyon, S. E., and Hoeppner, D. W. (Eds.), pp 17–32, West Conshohocken, PA, USA: ASTM International.

(25) Varenberg, M., Etsion, I., and Halperin, G. (2004), "Slip Index: A New Unified Approach to Fretting," *Tribology Letters*, **17**, pp 569–573. doi:10.1023/B:TRIL.0000044506.98760.f9

(26) Zhang, D., Shen, Y., Xu, L., and Ge, S. (2011), "Fretting Wear Behaviors of Steel Wires in Coal Mine under Different Corrosive Mediums," *Wear*, **271**, pp 866–874. doi:10.1016/j.wear.2011.03.028

(27) Goudreau, S., Charette, F., Hardy, C., and Cloutier, L. (1998), "Bending Energy Dissipation of Simplified Single-Layer Stranded Cable," *Journal of Engineering Mechanics*, **124**, pp 811–817. doi:10.1061/(ASCE)0733-9399(1998)124:8(811)

(28) Hong, K.-J., Der Kiureghian, A., and Sackman, J. L. (2005), "Bending Behavior of Helically Wrapped Cables," *Journal of Engineering Mechanics*, **131**, pp 500–511. doi:10.1061/(ASCE)0733-9399(2005)131:5(500)

(29) Martinez, M., Kante, R. B., Sicsic, P., and Cannell, D. (2017), "Two Scale Numerical Simulation of High Value Large Diameter Rope," *Proceedings of the OIPEEC Conference*, La Rochelle, France, 4–6 April 2017. Dohm, M. A. R. (Ed.), pp 313–330, St Martin d'Heres, France: OIPEEC.

(30) Raoof, M. (1990), "Simple Formulae for Spiral Strands and Multi-Strand Ropes," *Proceedings of the Institution of Civil Engineers Part 2*, **8**, pp 527–542. doi:10.1680/iicep.1990.11878

(31) Raoof, M. and Kraincanic, I. (1996), "Prediction of Axial Hysteresis in Locked Coil Ropes," *Journal of Strain Analysis for Engineering Design*, **31**, pp 341–351. doi:10.1243/03093247V315341

(32) Zhang, D.-K., Wang, S.-Q., Shen, Y., and Ge, S.-R. (2012), "Interactive Mechanisms of Fretting Wear and Corrosion of Steel Wires in Alkaline Corrosion Medium," *Proceedings of the Institution of Mechanical Engineers - Part J: Journal of Engineering Tribology*, **226**, pp 738–747. doi:10.1177/1350650112445852

(33) Bill, R. C. and Rohn, D. A. (1978), "Influence of Fretting on Flexural Fatigue of 304 Stainless Steel and Mild Steel," Washington DC, USA: National Aeronautics and Space Administration.

(34) Waterhouse, R. B. and Taylor, D. E. (1971), "The Initiation of Fatigue Cracks in a 0.7 Per Cent Carbon Steel by Fretting," *Wear*, **17**, pp 139–147. doi:10.1016/0043-1648(71)90024-X

(35) Jin, X., Shipway, P. H., and Sun, W. (2017), "The Role of Temperature and Frequency on Fretting Wear of a Like-on-Like Stainless Steel Contact," *Tribology Letters*, **65**, pp 1–15. doi:10.1007/s11249-017-0858-0

(36) Harris, S. J., Waterhouse, R. B., and McColl, I. R. (1993), "Fretting Damage in Locked Coil Steel Ropes," *Wear*, **170**, pp 63–70. doi:10.1016/0043-1648(93)90352-M

(37) Wang, D., Zhang, D., and Ge, S. (2012), "Effect of Displacement Amplitude on Fretting Fatigue Behavior of Hoisting Rope Wires in Low Cycle Fatigue," *Tribology International*, **52**, pp 178–189. doi:10.1016/j.triboint.2012.04.008

(38) Lombardini, L. (2017), "Verification of Rope Discard Criteria by Post Retirement Analysis," *Proceedings of the OIPEEC Conference*, La Rochelle, France, 4–6 April 2017. Dohm, M. A. R. (Ed.), pp 179–194, St Martin d'Heres, France: OIPEEC.

(39) Perier, V., Dieng, L., Gaillet, L., and Fouvry, S. (2011), "Influence of an Aqueous Environment on the Fretting Behaviour of Steel Wires Used in Civil Engineering Cables," *Wear*, **271**, pp 1585–1593. doi:10.1016/j.wear.2011.01.095

(40) Waterhouse, R. B. and Taylor, D. E. (1970), "The Relative Effects of Fretting and Corrosion on the Fatigue Strength of Eutectoid Steel," *Wear*, **15**, pp 449–451. doi:10.1016/0043-1648(70)90239-5

(41) Roche, V., Vanpeene, V., Rocha Prado, A. C., Nogueria, R. P., Pernot, S. (2017), "Preliminary Investigations of the Understanding of the Corrosion Mechanisms in Steel Wire Ropes," *Proceedings of the OIPEEC Conference*, La Rochelle, France, 4–6 April 2017. Dohm, M. A. R. (Ed.), pp 363–369, St Martin d'Heres, France: OIPEEC.

(42) Waterhouse, R. B. (2003), "Fretting in Steel Ropes and Cables—A Review," *Fretting Fatigue: Advances in Basic Understanding and Applications*, Mutoh, Y., Kinyon, S. E., and Hoeppner, D. W. (Eds.), pp 3–16, 4–6 April 2017. Dohm, M. A. R. (Ed.), ASTM International.

(43) Raoof, M. and Huang, Y.-P. (1991), "Upper-Bound Prediction of Cable Damping under Cyclic Bending," *Journal of Engineering Mechanics*, **117**, pp 2729–2747. doi:10.1061/(ASCE)0733-9399(1991)117:12(2729)

(44) McColl, I. R., Waterhouse, R. B., Harris, S. J., and Tsujikawa, M. (1995), "Lubricated Fretting Wear of a High-Strength Eutectoid Steel Rope Wire," *Wear*, **185**, pp 203–212. doi:10.1016/0043-1648(95)06616-0

(45) Shen, Y., Zhang, D., Duan, J., and Wang, D. (2011), "Fretting Wear Behaviors of Steel Wires under Friction-Increasing Grease Conditions," *Tribology International*, **44**, pp 1511–1517. doi:10.1016/j.triboint.2010.10.021

(46) Waterhouse, R. B., McColl, I. R., Harris, S. J., and Tsujikawa, M. (1994), "Fretting Wear of a High-Strength Heavily Work-Hardened Eutectoid Steel," *Wear*, **175**, pp 51–57. doi:10.1016/0043-1648(94)90167-8

(47) Llavori, I., Zabala, A., Otano, N., Tato, W., et al. (2019), "Development of a Modular Fretting Wear and Fretting Fatigue Tribometer for Thin Steel Wires: Design Concept and Preliminary Analysis of the Effect of Crossing Angle on Tangential Force," *Metals*, **9**, pp 1–11. doi:10.3390/met9060674

(48) Llavori, I., Zabala, A., Aginagalde, A., Tato, W., Ayerdi, J. J., and Gomez, X. (2020), "Critical Analysis of Coefficient of Friction Derivation Methods for Fretting under Gross Slip Regime," *Tribology International*, **143**. doi:10.1016/j.triboint.2019.105988

(49) Wang, D., Song, D., Wang, X., Zhang, D., Zhang, C., Wang, D., and Araujo, J. A. (2019), "Tribo-Fatigue Behaviors of Steel Wires under Couples Tension–Torsion in Different Environmental Media," *Wear*, **420–421**, pp 38–53. doi:10.1016/j.wear.2018.12.038

(50) Nishida, T., Kondoh, K., Xu, J. Q., and Mutoh, Y. (2003), "Observations and Analysis of Relative Slip in Fretting Fatigue," *Fretting Fatigue: Advances in Basic Understanding and Applications*, Mutoh, Y., Kinyon, S. E., and Hoeppner, D. W. (Eds.), West Conshohocken, PA, USA: ASTM International.

(51) Bhushan, B. (2002), *Introduction to Tribology*, Hoboken, NJ, USA: Wiley & Sons.

(52) Atkins, A. G. and Tabor, D. (1966), "The Plastic Deformation of Crossed Cylinders and Wedges," *Journal of the Institute of Metals*, **94**., Paper 2346, pp 107–115

(53) Williams, J. A. and Dwyer-Joyce, R. S. (2001), "Contact between Solid Surfaces," *Modern Tribology Handbook*, Bhushan, B. I. (Ed.), vol. 1, Section 3.2. London, UK: CRC Press.

(54) Meleddu, M., Foti, F., and Martinelli, L. (2017), "Temperatures in Active Heave Compensation Ropes," *Proceedings of the OIPEEC Conference*, La Rochelle, France, 4–6 April 2017. Dohm, M. A. R. (Ed.), pp 231–248.

(55) Hamilton, G. M. (1983), "Explicit Equations for the Stresses Beneath a Sliding Spherical Contact," *Proceedings of the Institution of Mechanical Engineers - Part C: Mechanical Engineering Science*, **197**, pp 53–59. doi:10.1243/PIME_PROC_1983_197_076_02

(56) D217-17. (2017), "Standard Test Methods for Cone Penetration of Lubricating Grease." West Conshohocken, PA, USA: ASTM International

(57) D937-07. (2012), "Standard Test Method for Cone Penetration of Petrolatum." West Conshohocken, PA, USA: ASTM International

(58) D1321-16a. (2016), "Standard Test Method for Needle Penetration of Petroleum Waxes." West Conshohocken, PA, USA: ASTM International

(59) Endo, H. and Marui, E. (2004), "Studies on Fretting Wear (Combinations of Various Ceramic Spheres and Carbon Steel Plates)," *Wear*, **257**, pp 80–88. doi:10.1016/j.wear.2003.10.018

(60) Maruyama, T., Saitoh, T., and Yokouchi, A. (2016), "Differences in Mechanisms for Fretting Wear Reduction between Oil and Grease Lubrication," *Tribology Transactions*, **60**, pp 497–505. doi:10.1080/10402004.2016.1180469

(61) Zhou, Z. R. and Vincent, L. (1999), "Lubrication in Fretting—A Review," *Wear*, **225–229**, pp 962–967. doi:10.1016/S0043-1648(99)00038-1